E3S Web of Conferences **504**, 02004 (2024) https://doi.org/10.1051/e3sconf/202450402004
Journées Scientifiques AGAP Qualité 2024

Stoneley wave detection by acoustic Interferometry: Estimation of shear velocity of a geological formation

Détection d'onde de Stoneley par interférométrie acoustique: estimation de la vitesse de cisaillement d'une formation géologique.

Jean Luc Mari[1, *] and Frederick Delay[2]

[1] Sorbonne Université, CNRS, EPHE, UMR 7619 METIS, 4 Place Jussieu, 75005, Paris, France, jeanluc90.mari@gmail.com

[2]ITES–UMR 7063, Department of Earth Sciences, University of Strasbourg, CNRS, ENGEES, F-67000 Strasbourg, France, fdelay@unistra.fr

Abstract. Both active and passive full waveform acoustic loggings (FWAL), complemented by a flow log, were conducted in a borehole of an experimental site located in the Cher region (France).. The acoustic tool used for the FWAL experiments is a flexible monopole tool holding a pair of piezoelectric receivers and a magnetostrictive transducer. The tool was modified to perform both active and passive FWAL. For passive acoustic logging, several runs were recorded to obtain a set of acoustic noise sections. As the noise is simultaneously recorded by two receivers of the tool, an interference noise section was elaborated by correlating or deconvolving the pair of signals and then summing these pairs of acoustic traces at each depth. This procedure, which can be interpreted as an interferometry analysis, points out the presence of low-frequency waves identified as Stoneley waves. The velocity and RMS amplitude of the Stoneley wave were computed at each depth. It is shown that: 1- the Stoneley wave velocity obtained in passive mode can be used to estimate the shear velocity of the formation, 2- the RMS amplitude and velocity variations of the Stoneley waves are strongly correlated with the variations of the flowmeter.

Une diagraphie en champ total, active et passive, a été enregistrée dans un forage d'un site experimental situé dans la région du Cher (France). Dans le forage un débitmètre a été enregistré. L'outil acoustique utilisé est un outil monopole flexible comprenant une paire de récepteurs piézoélectriques et un émetteur magnétostrictif. L'outil a été modifié pour faire des mesures en actif et en passif. Pour la diagraphie acoustique passive, plusieurs runs ont été enregistrés et obtenir ainsi un ensemble de profils de bruit acoustique. Le bruit étant simultanément enregistré par deux récepteurs de l'outil, une section d'interférence de bruit a été obtenue par corrélation ou déconvolution puis par sommation des paires de traces acoustiques à chaque profondeur. Cette procédure qui peut être interprétée comme une analyse interférométrique, met en évidence la présence d'onde de Stoneley. La vitesse et l'amplitude de l'onde de Stoneley sont mesurées à chaque profondeur. Il est montré que : 1- la vitesse de l'onde de Stoneley obtenue en mode passif peut être utilisée pour estimer la vitesse de cisaillement de la formation, 2- les variations d'amplitude et de vitesse de l'onde de Stoneley sont fortement corrélées aux variations du débitmètre.

*Corresponding author: jeanluc90.mari@gmail.com

1 Introduction

Full waveform acoustic logging (FWAL) and vertical seismic profile (VSP) were conducted over two boreholes from an experimental site in the Cher region (France). The site was also investigated (from the surface) by hybrid seismic imaging. The acoustic tool was modified to allow for passive monitoring in addition to more classical active measurements. To our knowledge, performing both passive and active acoustic loggings over the same well is a novelty which reveals how both types of signals can be used for characterizing a geological formation, mainly regarding mechanical parameters such as acoustic velocities and Poison's ratio.

Active acoustic logging is a common and relatively well-established practice [1, 2] used to determine the P-wave velocity (VP) of a formation. Full Wave Form Acoustic logging (FWAL) is the record of acoustic waves propagated in a borehole between one or more sources and one or more receivers housed by the same logging tool. Either monopole or dipole tools with multidirectional transmitters and receivers can be used, the monopole being the most employed. In a borehole filled with fluid or mud, the transmitters generate a compression wave, which converts in the formation into a refracted compression wave (P-wave) and a refracted shear wave (S-wave) at the refraction limit angles. The converted refracted shear wave exists only if the shear velocity of the formation is larger than the P-wave velocity in the mud, the geological formation being said a fast formation. In the opposite, the formation is said slow. The measurement of arrival times for both the refracted P-waves and the converted refracted S-waves (fast formation), recorded by at least two adjacent receivers of the acoustic tool give the P-wave and S-wave velocities (VP and VS) of the geological formation.

In a vertical well, monopole tools can enable the recording of five propagation modes as: refracted compression waves, refracted shear waves (only in fast formations), fluid waves, and two dispersive guided modes as pseudo-Rayleigh waves (in fast formations), and Stoneley waves.

In fast formations, a simple monopole tool records a converted refracted S-wave, which then gives the shear velocity of the formation. In slow formations, a dipole tool should be used. Dipole acoustic tools are equipped with polarized transmitters and receivers generating and recording compression waves perpendicular to the borehole direction. These compression waves generate flexure modes at the borehole wall that induce pseudo-shear waves (flexural waves) in the formation propagated parallel to the borehole direction. Dipole tools are also used to evaluate the anisotropy of the formation by studying the phenomenon of shear wave splitting [3].

An alternative approach to measure the shear velocity of a formation is to analyze the Stoneley waves. Stoneley waves are dispersive interface waves. The shear velocity of the formation can be estimated indirectly from the Stoneley wave dispersion equation [4]. At low frequencies, Stoneley waves are analogous to tube waves observed in a VSP.

FWAL, based on the analysis and processing of the various wave trains (refracted waves, guided waves, reflected waves) recorded by an acoustic tool, provides detailed information on a borehole as a function of depth, in terms of acoustic wave velocities and rock petrophysical characteristics [5], detection of geological features such as fractured zones, karstic bodies [6] or preferential flow zones [7].

Flows can also be detected using ambient noise measurement, FWAL, and VSP data recorded with a hydrophone sensor [8]. More recently, a source-free distributed-acoustic-sensing (DAS) logging method based on borehole ambient noise monitoring has been introduced [9]. The receivers of the source-free DAS logging tool are fiber optic cables cemented between the casing and the wellbore. The ambient noise root-mean-squared (RMS) amplitudes correlate well with anomalies revealed by conventional logging data. The feasibility of a source-free DAS logging was evaluated by analysing a borehole DAS ambient noise dataset collected at the Frontier Observatory for Research in Geothermal Energy site in Utah. The borehole DAS ambient noise was collected within the granitic basement rock using a 1-km optic fiber cable cemented in the narrow interspace between casing and wellbore of a vertical observation well. The RMS noise amplitudes were computed to construct a profile showing RMS still varying over depth, with a few peaks at several distinct depths. By comparing the noise RMS profile with available logging data, a clear correlation appeared between major RMS peaks and low-velocity layers (LVL) bounded by sharp structural interfaces. It was also found that the noise RMS amplitude peak zones were only correlated with LVLs associated with both low Poisson's ratio and high porosity, indicating highly fractured zones [9].

2 Geophysical investigations at the Apec site: an example

The experimental site investigated in this study is located in the Cher region (France) at the transition from Triassic to Jurassic geological formations, partly overlaid by thin superficial formations. The sedimentary formation is mainly composed of limestone up to 120 m depth and sandstones with some argillite and dolomite intercalations between 120 m and 200 m. The site was investigated from the surface via hybrid seismic imaging and from two boreholes (B1 and B2, Fig. 1) via FWAL and VSP [10]. Borehole B1, drilled up to a depth of 90 m, is fully steel cased and cemented. Borehole B2, drilled up to a depth of 200 m, is steel cased and not cemented up to 78 m then equipped with a slotted PVC casing between 78 and 200 m. Borehole B2 was cored in the 78 – 200 m depth interval. A lithological column was obtained in B2 by core description. A VSP was recorded in borehole B1 along the 25 -90 m depth interval (Fig. 1a), and FWAL were conducted both in boreholes B1 and B2.

A seismic line was also recorded at the site with a seismic spread composed of 48 fixed geophones (2 m lag distance between neighbors, Fig. 1a), while the source, as a weight dropper (Fig. 1a), was moved and fired in the middle of all pairs of adjacent geophones. Hybrid seismic imaging combining refraction (tomography, Fig. 1a) and reflection seismic results produced an extended depth reflectivity section starting from the surface up to a depth of 240 m (Fig. 1b). Time to depth conversion was calculated using the time - depth law given by the VSP recorded in borehole B1 [10].

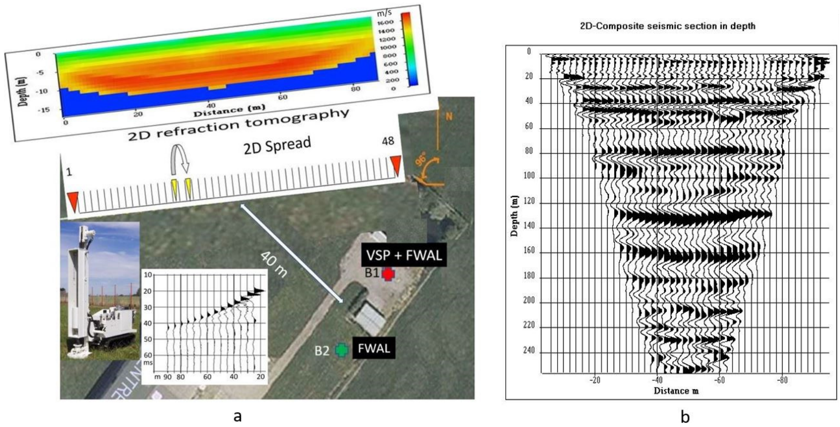

Fig. 1. *Seismic imaging: (a) 2D seismic spread – 2D refraction tomography, borehole locations (B1 and B2), view of the seismic source, VSP recorded in B1, (b) 2D hybrid section over depth. After [10].*

3 Active acoustic logging

The acoustic tool used for the FWAL experiments is a flexible monopole tool holding a magnetostrictive transmitter (transmission frequencies: 17-22 kHz) and a pair of piezoelectric receivers offering an acquisition in far offset configuration (receivers 3 and 3.25 m beneath the source). The tool was modified to perform both active and passive FWAL. In active mode, the logging speed was 5m/min, and the acquisition parameters were set up as: a depth sampling interval of 5 cm, a time sampling interval of 5 µs, and a recording length of 5 ms.

Borehole B2 being steel cased but not cemented in the upper part, strong resonances are observed on the acoustic sections. Consequently, acoustic data recorded in borehole B1 (steel cased hole) in the 30-78 m depth interval have been merged with acoustic data recorded in borehole B2 (slotted PVC cased hole) in the 78-192 m depth interval to obtain a composite acoustic section (Fig. 2). Acoustic data were processed to obtain a very high-resolution velocity log (Fig. 2) which was used as a constraint to transform the seismic section into pseudo-velocities. After calibration, and under the assumption that the slower the wave velocity, the higher the permeability – porosity, the seismic line informs on preferential areas where flow should occur. At the scale of an open wellbore, acoustic loggings reporting on wave velocities over a short distance within the well, also inform on open features crosscut by the borehole. The velocity distribution has been converted into porosity using the Raymer equation adapted to carbonate formation. The results are shown within the 30-190 m depth interval in Figure 2, with high-porosity layers appearing in red.

 https://doi.org/10.1051/e3sconf/202450402004

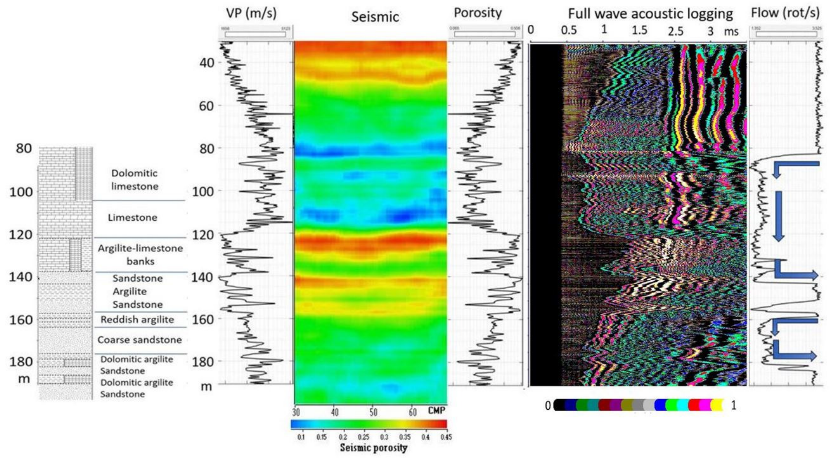

Fig. 2. *Seismic imaging and active acoustic logging: from left to right: lithological column, acoustic velocity, seismic section converted in porosity, acoustic porosity, Full wave acoustic composite section (0 -80 m: borehole B1, 80 – 190 m: borehole B2 slotted PVC cased hole) and flowmeter. After [10].*

A flow meter was recorded in borehole B2 (Fig. 2). Flow-log measurements were performed with a downward moving probe at constant speed corresponding to a constant rotation of the propeller of the flowmeter, the rotation speed being on the order of 3.3 rotations/second. The flowmeter measurements evidence that water flows from the formation into the well at 83-85 m depth, then flows downward into the well and goes back into the formation at 143 m. The same geometry of flow occurs between 152 to 156 m, and then from 159 m to 181-183 m. The water "loops" are indicated by blue arrows on the flow log, the arrows also pointing out that the Stoneley waves (between 2.5 and 3.5 ms on the FWAL, in Fig. 2) are strongly attenuated at the depths of water loops. Flows is also witnessed by low velocity levels corresponding to high porosity horizons.

4 Passive acoustic logging in borehole B2

In passive mode, the transducer is inactivated. The logging speed is 2 m/min. The acquisition parameters are; the depth sampling interval: 1 cm, time sampling interval: 10 µs, and recording length: limited to 10 ms, due to the acquisition device. Four runs were recorded in the passive mode to obtain a set of acoustic noise sections, with two runs in the downward direction and two in the upward direction. The acoustic noise sections were resampled at a depth sampling interval of 5 cm, Figure 3a giving the passive acoustic data between 80 and 180 m depth in well B2 for 10 ms of recording duration at each depth.

In a well the "fluid induced ambient noise" is mainly driven by the interactions between the well and the formations. The ambient noise records can be governed by well design (varying diameter), mud invasion, borehole wall damage, and the quality of the cement bond. However, when not adversely affected by the well conditions, the distribution of noise frequencies and noise RMS are correlated to geologic properties like transmissive fractures, permeability, P-wave velocity, porosity, and can thus be used to infer lithology.

A previous ambient noise analysis [11] showed that:

- the variations of the noise RMS amplitude log (Fig. 3b) are consistent with both the variations of the P-wave velocity log and the lithological column.
- the distribution of noise frequencies in the 0 -5 kHz bandwidth (Fig. 3c) is strongly correlated with the variations of the flowmeter, with an increase of noise frequency and noise amplitude where flow loops occur in the well (Fig. 3d).

As the noise is simultaneously recorded by two receivers of the tool, an interference noise section was constructed by correlating and summing pairs of acoustic traces at each depth, the correlation being done between the noise recorded by the first receiver and the noise recorded by the second receiver, 0.25 m away from the first receiver. This procedure can be seen as an interferometry analysis [12]. The correlation is calculated at each depth by Fourier transform. The cross-correlation sections computed for each run (4 runs being recorded) were stacked to obtain the interference noise section (Fig. 4a). The causal part of the interference section is associated with correlation over positive times and the acausal part with correlation over negative times, those times corresponding to up-going and down-going wave fields, respectively.

The presence of events, coherent between two receivers but delayed in time (not located at the same relative time zero) and with significant amplitude, indicates that acoustic waves are propagating in the borehole. Such events, indicated by red arrows in Figure 4a, can be seen in the interference noise section. The phenomenon is better evidenced in the causal part of the interference noise section. As the events exist both in the causal and acausal parts of the interference noise sections, the wave propagation occurs in both directions, downward and upward, in the borehole. However, it is well known that changes in the frequency content of the sources may affect the apparent velocity and amplitude of the reconstructed phases. To compensate for the effects of the source variations (noise recorded by the first receiver), the operation of correlation has been replaced by a deconvolution. Hence, the interference acoustic noise section was constructed by deconvolution and summing pairs of acoustic traces at each depth, the deconvolution being done between the noise recorded by the first receiver and the noise recorded by the second receiver, 0.25 m away from the first receiver (Fig. 4b). After deconvolution and sum (of the four profiles), the resulting acoustic wave field is mainly restricted to the direct arrival phase at 0.2 ms (the most energetic phase) with two maxima of energy located at depths of 140-151m and 153-158m (yellow spots in the band 0.2 ms in Fig. 4b)

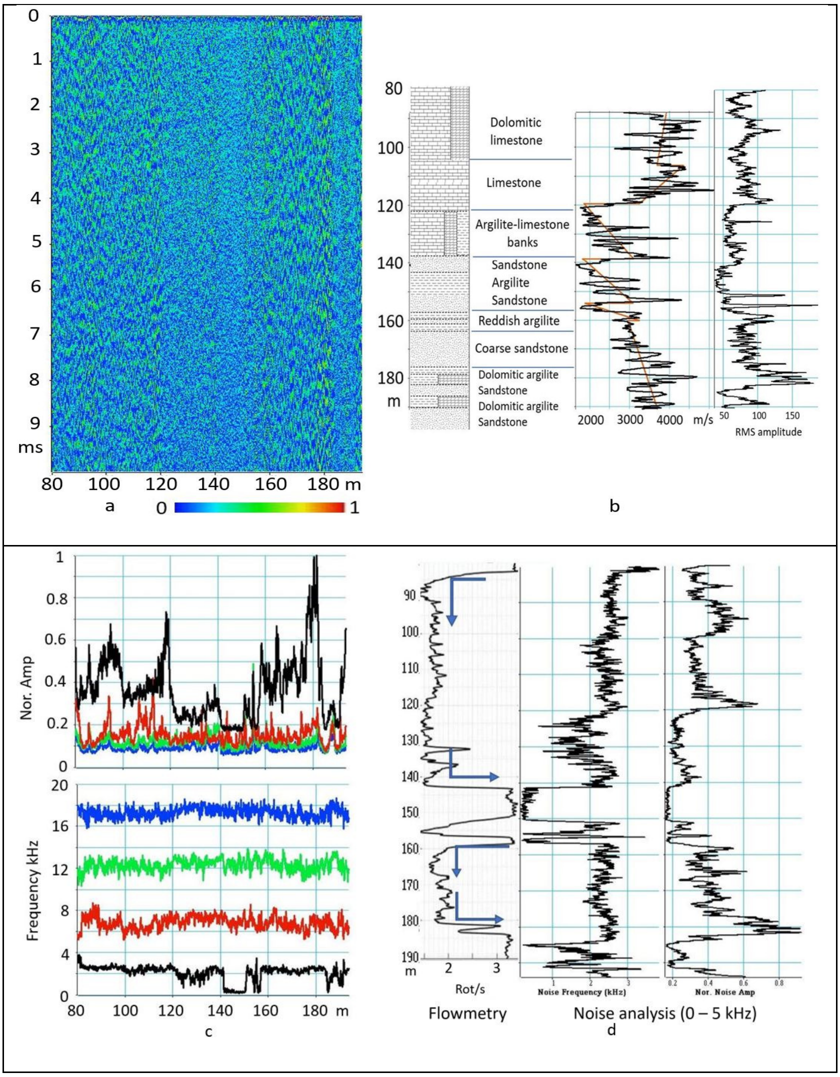

Fig. 3. *Passive acoustic logging in borehole B2. Noise section (a), P-wave velocity log (active acoustic logging) and noise RMS amplitude log (b). Noise analysis in different frequency bandwidths (0-5 kHz (black curve), 5-10 kHz (red curve), 10-15kHz (green curve), 15-20 kHz (blue curve)): Noise spectral amplitude logs and, Noise frequency logs (c). Passive acoustic logging versus flowmetry. From left to right: flowmeter, frequency log and spectral amplitude log in 0 -5 kHz from noise analysis (d). After [11].*

 https://doi.org/10.1051/e3sconf/202450402004

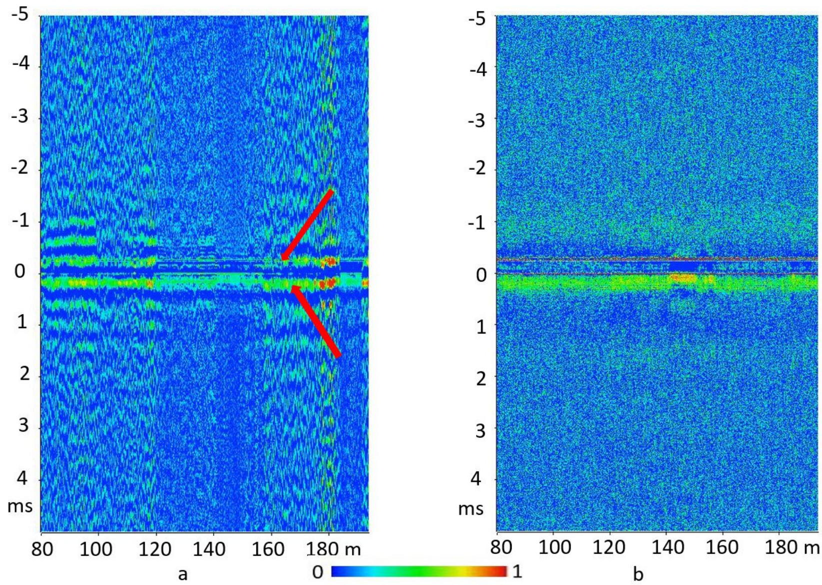

Fig. 4. *Passive acoustic logging processed by interferometry.*
a: interference noise section obtained by correlation. b: interference noise section obtained by deconvolution. The sections are normalized and displayed with a color scale ranging from 0 (blue) to 1 (red). Arrows indicate the presence of acoustic waves.

Figure 5a shows a zoom of the causal part of the interference noise section (obtained by deconvolution) in the 0 – 2.5 ms time interval, where the acoustic wave is clearly visible. Picking the maximum amplitude of the interference section gives the (statistical) transit times DTmax of the acoustic wave between the two receivers (0.25 m lag distance) of the acoustic tool. The picked times are used to flatten the interference noise section (Fig. 5b). A correct flattening of the interference section with the picked DTmax guarantees an accurate selection of those transit times. The picked times DTmax were used to obtain a log of propagation velocity V-DTmax of the acoustic wave, as well as a normalized energy log (Fig.5a). The normalized energy log shows major peaks of energy at depths of 140-151m and 153-158m. The variations of velocity and normalized energy logs point out different noise units: 80-120 m depth, 120-140 m, 140-151 m, 151-153 m, 153-158 m, 158-175 m, and 175-194 m (Fig. 5b). The noise units are consistent with the lithological column. The acoustic wave identified by interferometry has a propagation velocity varying between 890 m/s and 1540 m/s, with an average value of 1170 m/s associated with a standard deviation of 140 m/s. The range of velocities identifies the detected wave as a Stoneley wave. It can also be noticed that high values of velocity are associated with high values of energy, as the example in the 151 – 158 m depth interval.

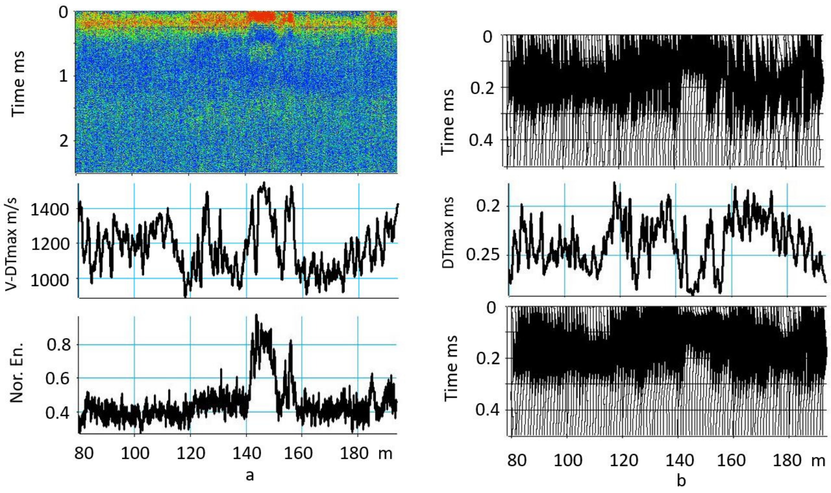

Fig. 5. *Passive acoustic logging: Identification of a Stoneley wave.*
a: causal part of the interference noise section in the 0 - 2.5 ms interval (the section is normalized and displayed with a color scale ranging from 0 (blue) to 1 (red)) and acoustic logs: velocity (V-DTmax) and normalized energy log.
b: from top to bottom: zoom of the interference noise section in 0 - 0.5 ms time interval, picked times DTmax of the maximum of the interference noise section, flattening of the interference noise section with DTmax.

The Stoneley wave can be used to estimate the shear velocity VS of the formation from the Stoneley wave dispersion equation [4]. According to White [13], VS can be derived from a simplified version of the dispersion equation relating the shear-wave velocity (VS), the low-frequency Stoneley velocity (VSt), the fluid velocity (Vf), and formation and fluid densities (ρ and ρ_f, respectively):

$$\frac{1}{V_{St}^2} - \frac{1}{V_f^2} = \frac{\rho_f}{\rho} \cdot \frac{1}{V_S^2}$$

As no density log is available, an estimation of ρ can be given by a Gardner equation: $\rho = \alpha VP^{\beta}$, with α and β scalar coefficients, here prescribed at 0.3 and 0.25, respectively. The shear velocity (VS) estimation from Stoneley-wave velocity is done under specific constraints: VS < 0.65×VP and 0.2 < Poisson's ratio < 0.45. The results are shown in Figure 6. The shear velocity log, noted VS-St in Figure 6 to remind that the shear velocity is estimated from Stoneley wave velocity, varies between 980 m/s and 2080 m/s, with an average value of 1540 m/s associated with a standard deviation of 270 m/s. The associated Poisson's ratio log varies between 0.23 and 0.39, with an average value of 0.34 associated with a standard deviation of 0.04. We can also notice a very high correlation (0.98) between the Poisson's ratio and the VP to VSt ratio, suggesting that the latter could be used as pseudo-Poisson's ratio indicator. We can also notice that the lowest values of these two logs are in the 140-158 m depth interval, suggesting a compacted formation although the P-wave velocity of the formation is low (2000 m/s).

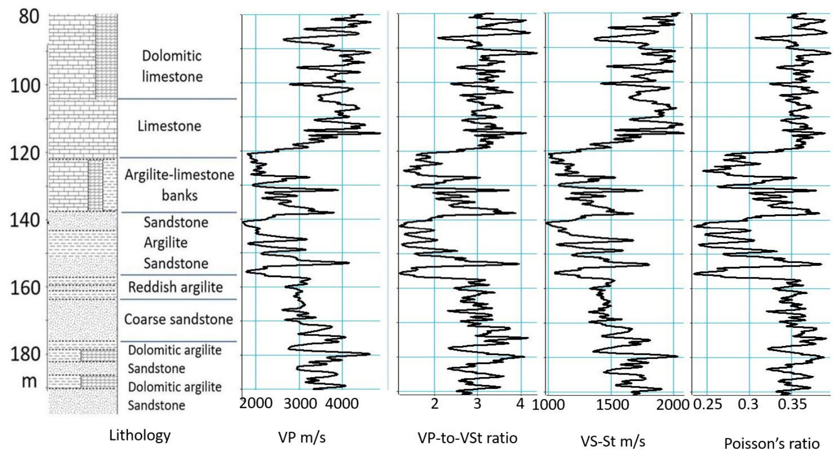

Fig. 6. *Passive acoustic logging: Shear velocity estimation.*
From left to right: lithology, P-wave velocity, P-wave velocity to Stoneley wave velocity ratio, S-wave velocity VS-St estimated from Stoneley wave dispersion equation, Poisson's ratio.

Notably, the efficiency of the interferometry process could be enhanced by increasing the number of experiments (here runs). For that purpose, the acquisition of ambient noise could be done simultaneously on several receivers of an acoustic tool and also by increasing the record duration.

5 Discussion

When a fluid is moving through or along a medium it produces an acoustic noise stemming from both the fluid itself and vibrating elements streamlined by flow. The fluid noise is the result of internal friction, usually audible in highly turbulent flows, with a noise spectrum strongly depending on the fluid type, pressure, temperature, and flow rate. Notably, different types of rocks generate acoustic noise in different frequency bandwidths [14].

The acoustic logs obtained from passive acoustic interferometry were compared with P-wave acoustic velocity, core data and flowmetry. The interpretation of passive acoustic data processed by interferometry renders the two following main sets of results.

- Processing the passive acoustic data by interferometry (seeking deconvolution between two signals collected at a short lag distance) allows for reconstructing an acoustic wave identified as a Stoneley wave, the velocity of which can be used to estimate the shear velocity of geological formations crosscut by drilling.
- the distribution of Stoneley velocity and energy (squared RMS amplitude) variations are strongly correlated with the variations of the flowmeter (Fig.

 https://doi.org/10.1051/e3sconf/202450402004

7, the levels of in-flows or out-flows are indicated by blue arrows on the flowmeter). The flows observed at different depth intervals (83-143 m, 152-156 m, and 159-181 m) are characterized by both a sharp decrease in the rotation of the propeller of the flowmeter, and a complete independence over depth of the flow loops, those being well-separated by segments where no flow occurs in the well. The phenomenon is clearly associated with a strong decrease of the energy of the Stoneley wave where flow loops occur in the well.

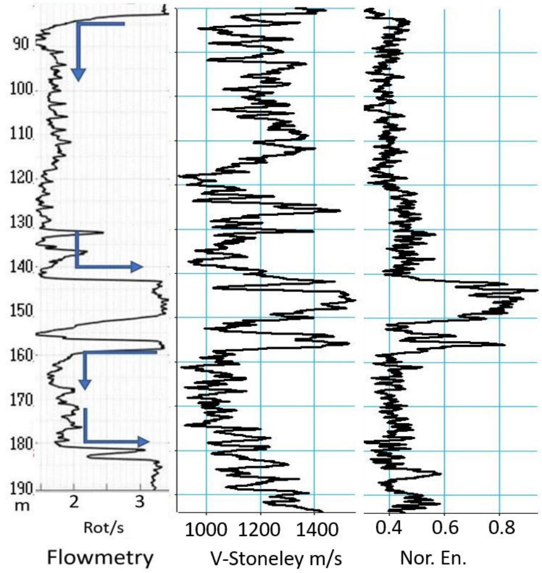

Fig. 7. *Passive acoustic logging: Stoneley-wave properties vs flowmetry*
From left to right: Flowmetry, Stoneley-wave velocity, and normalized noise energy logs.

The results obtained (decrease of both energy and velocity of the Stoneley wave) are consistent with the results which could be obtained by a Biot-Rosenbaum model [4,15] used to access to permeability from the evolution of Stoneley's phase velocity and attenuation [16].

6 Conclusion

APEC (Association Pédagogique et Expérimentale du Cher) has developed a site for the training in applied geophysics of both students and professionals. Two boreholes are available at the site. The site is currently used for experimental studies in near surface geophysics and logging.

An acoustic logging tool was modified to conduct both passive and active acoustic monitoring. The paper has been focused on passive acoustic logging. The field example has shown that ambient noise recorded simultaneously on 2 receivers of an acoustic tool, over short time windows (limited to 10 ms due to the acquisition device) and with a limited number of experiments (4 runs) can be processed by interferometry to detect the propagation of a Stoneley wave and to estimate its properties (propagation velocity and energy).

In interferometry, the noise recorded by the first receiver is acting as a source for the noise recorded by the second receiver. It has been shown the benefit of replacing the operation of noise correlation between the two receivers by a deconvolution which compensates for the effects of source variations in the computation of interference sections.

Notably, the efficiency of the interferometry process could be enhanced by increasing the number of experiments (here runs in a well). The acquisition of ambient noise simultaneously on several receivers of an acoustic tool would provide data redundancy without significantly increasing the acoustic logging time. As an example, passive acoustic data could be recorded when the acoustic tool is run downward and active acoustic data when the tool is run upward.

By integrating active and passive acoustic logging, operators can gain a more holistic view of the reservoir. The combined data could help identifying formation heterogeneity, fluid distribution, connectivity between reservoir zones, and the presence of geologic features as faults or fractures.

In this context, both Spectral Noise Logging (SNL) and borehole interferometric tomography are applications where DAS could be extremely valuable as a passive acoustic logging and monitoring system. The combination of active sonic logging survey and passive DAS monitoring could offer synergistic benefits by leveraging the strengths of each technique. One can imagine a conventional sonic system with a hybrid copper-fiber cable allowing for a sonic source to calibrate DAS records aimed at providing SNL and ambient noise tomography over time.

Acknowledgements

We thank APEC (Association Pédagogique et Expérimentale du Cher) for granting us the permission to use full waveform acoustic data and logging data.

Special thanks to Pierre Gaudiani for the modification of the acoustic tool and the acquisition of acoustic data.
Special thanks to Christophe Voisin and Thomas Kremer (Geolinks) for useful discussions, regarding the processing of passive acoustic data.
Special thanks to Christophe Maisons (Febus-optics) for suggesting the idea of combining active sonic logging survey and passive DAS monitoring.

Funding

The authors acknowledge financial support from APEC.

References

1. G. C. Summers, R.A. Broding, (1952), Continuous Velocity Logging, Geophysics, 17, pp.598-614.
2. C.B. Vogel, (1952), A seismic logging method, Geophysics, 17, pp. 579-586.
3. J. Perrin, D. Belaud, J.P. Yver, C. Naville, (2022), S-wave anisotropy from two dipole sonic data processing methods confronted with fracture permeability, logs and cores, Science and Technology for Energy Transition, Volume 77, https://doi.org/10.2516/stet/2022006
4. M.A. Biot, (1952), Propagation of elastic waves in a cylindrical borehole containing fluid. Journal of Applied Physics, 223, 997-1005.
5. B. Benjumea B., A.I. Lopez, J.L. Mari, J.L. Garcia-Lobon, (2018), Petrophysical characterization of carbonates (SE of Spain) through full wave sonic data, Journal of applied geophysics, 160, 1-14,

   https://doi.org/10.1016/j.jappgeo.2018.10.024
6. J.L. Mari, G. Porel, F. Delay, Contribution of Full Wave Acoustic Logging to the Detection and Prediction of Karstic Bodies, *Water* **2020**, *12*(4), 948; doi:10.3390/w12040948.
7. F. Delay, J.L. Mari, G. Porel, F. Chabaux, P. Ackerer, (2022), Is subsurface geophysics as seismic and acoustic investigations a rescue to groundwater flow inversion? , Comptes Rendus Geoscience, Part of Special Issue: Geo-hydrological data & models ,https://doi.org/10.5802/crgeos.157.
8. J.L. Mari, G. Porel, (2016), Flow detection using well seismic data, 78th EAGE Conference & Exhibition 2016, Vienna, Austria, 30 May – 2 June 2016.
9. D. Li, L. Huang, Y. Zheng, Y. Li, P. Wannamaker, J. Moore, (2022), Feasibility of source-free DAS logging for next-generation borehole imaging, Scientific reports, https://doi.org/10.1038/s41598-022-16027-3.
10. J. L. Mari, F. Delay, G. Porel, P. Gaudiani, (2021), Characterizing flow in the first hundred-meter depth of a fractured aquifer using hybrid seismic methods, acoustic logging, and flow log measurements, Oil & Gas Science and Technology – Rev. IFP Energies Nouvelles **76**, 62, https://doi.org/10.2516/ogst/2021048,
11. J. L. Mari, F. Delay, C. Voisin, P. Gaudiani, (2023), Active and passive acoustic logging applied to the detection of preferential flow in a sedimentary aquifer, Science and Technology for Energy Transition, Volume ??, https://doi.org/10.2516/stet/2023018.
12. G. D. Bensen, M. H. Ritzwoller, M.P. Barmin, A.L. Levshin, F. Lin, M.P. Moschetti, N. M. Shapiro, Y. Yang, (2007), Processing seismic ambient noise data to obtain reliable broad-band surface wave dispersion measurements, Geophysical Journal International, Volume 169, Issue 3, pp 1239 -1260, https://doi.org/10.1111/j.1365-246X.2007.03374.x

13. J. E. White, (1983), Underground sound – Application of Seismic Waves. Elsevier, Amsterdam, Oxford, New York.
14. A. Aslanyan, D. Davydov, (2012), Spectral Noise Logging, Technical overview, TGT Oilfield Services, www.tgtoil.com
15. J. H. Rosenbaum, (1974), Synthetic microseismograms: logging in porous formation, Geophysics, 39, 14-32.
16. K. Khayer, Adel Shirazy, Aref Shirazy, A. Ansari, A. Hezarkhani, (2022), Permeability estimation from Stoneley waves in carbonate reservoir, Geological Bullin of Turkey, 65 – 42, doi: 10.25288/tjb.974505.